Vol. 82: 19–29, 2018
https://doi.org/10.3354/ame01880

AQUATIC MICROBIAL ECOLOGY
Aquat Microb Ecol

Published online August 31

Altering phytoplankton growth rates changes their value as food for microzooplankton grazers

Kelsey A. McBeain[1,2], Kimberly H. Halsey[1,*]

[1]Department of Microbiology, Oregon State University, Corvallis, Oregon 97331, USA

[2]*Present address:* Ecology, Evolution and Marine Biology, University of California, Santa Barbara, California 93106, USA

ABSTRACT: When microzooplankton graze phytoplankton prey, the consumed carbon is partitioned into particulates, dissolved organic carbon (DOC), and CO_2. Allocation of prey carbon to these various fates has important consequences for marine ecosystem function. A 2-stage continuous culture system was used to investigate carbon allocation by microzooplankton consuming phytoplankton grown in chemostats at controlled, nutrient-limited growth rates. The chemical composition of *Dunaliella tertiolecta* and *Thalassiosira pseudonana* cells varied with growth rate. When a constant amount of prey carbon was fed to the dinoflagellate *Oxyrrhis marina*, the carbon transfer efficiency to particulates (CTE) decreased from 27 ± 5% when fast-growing *T. pseudonana* cells were the prey to only 3 ± 2% when slow-growing cells were the prey. DOC did not increase with decreasing CTE, indicating that an increase in CO_2 remineralization caused the lower CTE when the slow-growing cells were consumed. A similar pattern was observed when *D. tertiolecta* was the prey, but CTE was higher: 42 ± 15% for fast-growing cells, declining to 17 ± 6% for slow-growing prey cells. The microzooplankter showed greater neutral lipid accumulation when fed *D. tertiolecta*; however, its neutral lipid content did not necessarily mirror that of its phytoplankton prey and varied substantially across treatments. These findings demonstrate that microzooplankton respond strongly to food qualities of prey cells that are influenced by growth rate. We conclude that a significant and variable portion of primary production is lost from ecosystems because microzooplankton CTE is strongly influenced by the impacts of nutrient limitation on prey growth rates.

KEY WORDS: Microzooplankton · Nutrient-limitation · Food quality · Phytoplankton growth rate · Predator–prey dynamics

INTRODUCTION

Microzooplankton consume 50 to 80% of ocean primary production every day (Calbet & Landry 2004). The immediate fate of the consumed phytoplankton carbon is assimilation into particulate organic matter, including microzooplankton biomass and egested fecal pellets, excretion as dissolved organic carbon (DOC), and remineralization back to CO_2. The relative allocation of carbon to these fates has significant consequences for marine food-web dynamics, microbial community composition, and carbon sequestration into the deep ocean biome (Anderson et al. 2013). Carbon transfer efficiencies (CTEs) quantify the fraction of prey carbon assimilated into the next trophic level (microzooplankton biomass) and/or made available for export out of the euphotic zone (egested fecal pellets). The efficiency with which bacterial carbon is incorporated into grazer biomass varies from ~2 to 80% and is thought to be largely dependent on prey nutritional state (Caron & Hutchins 2013). High CTEs support a strong biological carbon pump, and low CTEs are generally associated with rapid carbon remineralization back to CO_2, thus limiting long-term carbon sequestration.

*Corresponding author: halseyk@science.oregonstate.edu

Marine ecosystem models rely on predictions of plankton responses at the base of the food web to changing environmental conditions to achieve fidelity in representing the dynamic states of real systems. In marine ecosystems, phytoplankton productivity is frequently nutrient-limited. For example, during months of seasonal stratification in the low-nutrient environments of the oligotrophic gyres, primary production is largely maintained through remineralization of nitrogen. Chemostat cultures are widely used to evaluate the responses of cells to nutrient-limited growth. In a chemostat, cells are maintained at a constant growth rate that is defined by the dilution rate and volume of the culture (reviewed in Bull 2010). About 7 to 10 cell divisions are required before cells in a chemostat are fully acclimated to their environment and their growth-rate-dependent physiology can be studied (Cullen et al. 1992). This culturing technique has been used to show the remarkable physiological plasticity exemplified by phytoplankton that were acclimated to different nutrient-limited growth rates. For example, phytoplankton C:N and the ratio of carbon to chlorophyll (C:Chl) vary about 3-fold depending on nutrient-limited growth rate (Rhee 1978, Herzig & Falkowski 1989, Chalup & Laws 1990, Geider & La Roche 2002, Halsey et al. 2010, 2014) or across a day–night cycle (Halsey et al. 2013, Lopez et al. 2016).

Nutrient-limited growth rate also impacts phytoplankton macromolecular composition (Shuter 1979, Morris 1980, Halsey et al. 2011). During steady-state growth (Cullen et al. 1992, MacIntyre & Cullen 2005), phytoplankton carbon is increasingly directed to carbohydrates as nitrogen becomes more limited, and to lipids as nitrogen becomes more available (Halsey et al. 2011, Halsey & Jones 2015). However, carbon partitioning can be species-specific (Shifrin & Chisholm 1981, Bi et al. 2014). The overall caloric content of phytoplankton carbon is also quite flexible because of the fundamental differences in the biochemical reduction states of carbohydrates and lipids. Studies of the dietary quality of phytoplankton as prey have focused primarily on their elemental composition (Sterner & Elser 2002, Jones & Flynn 2005, Andersen et al. 2007, Golz et al. 2015) and presence of certain essential fatty acids (Chu et al. 2008, 2009, Lund et al. 2008). Cellular elemental composition is related to macromolecular composition (Klausmeier et al. 2004), but C:N:P does not take into account the energetic qualities of different carbon pools that could be used by microzooplankton to sustain growth.

Microzooplankton are thought to have less physiological plasticity than their phytoplankton prey. To achieve elemental stoichiometric (C:N:P) homeostasis, microzooplankton alter their ingestion, egestion, and respiration rates (Frost et al. 2005, Meunier 2012). For example, respiration rates in heterotrophic protists were significantly higher when fed nitrogen-starved phytoplankton (cells with high C:N ratios) compared to nitrogen-replete phytoplankton (cells with low C:N ratios) (Darchambeau et al. 2003, Hantzsche & Boersma 2010). However, the influence of phytoplankton carbon composition on microzooplankton physiology has received less attention.

In this study, we aimed to determine whether growth-rate-dependent differences in phytoplankton composition influence carbon allocation in the model heterotrophic microzooplankter *Oxyrrhis marina*. We employed a rarely used technique, 2-stage continuous culture (Curds & Cockburn 1971), that uses the output from one chemostat as input to a second chemostat. We assessed (1) whether *O. marina* was able to maintain stable growth while being fed a constant diet of either the green alga *Dunaliella tertiolecta* or diatom *Thalassiosira pseudonana* that were grown at varying nutrient-limited growth rates, (2) CTEs and nitrogen transfer efficiencies (NTE) of prey carbon into *O. marina* particulates, and (3) how neutral lipid accumulation in the prey compared to that in *O. marina*. The results showed that phytoplankton growth rate has major impacts on the fate of phytoplankton carbon consumed by *O. marina*. Our findings suggest that expanding regions of nutrient limitation in the open ocean could significantly alter marine food-web structure and weaken the biological carbon pump.

MATERIALS AND METHODS

Cultures and growth conditions

Phytoplankton prey species *Dunaliella tertiolecta* CCMP1320 and *Thalassiosira pseudonana* CCMP1335 were obtained from the National Center for Marine Algae and Microbiota (NCMA) and maintained in f/2 medium (Guillard 1975). Stock cultures were grown in constant light at 60 to 65 µmol photons m^{-2} s^{-1} at 18°C. The microzooplankter *Oxyrrhis marina* CCMP1788 was obtained from NCMA and maintained in stock cultures inoculated with *D. tertiolecta* or *T. pseudonana* at a ratio of 1 *O. marina* cell to 500 prey in modified f/50 medium (medium contained only 4 µM nitrate; see below). Cultures were kept in the dark at 18°C.

Continuous cultures of either *D. tertiolecta* or *T. pseudonana* (0.3 l) were maintained in the first stage of a 2-stage continuous culture system in modified f/2 (to ensure that nitrate was the limiting nutrient, the medium contained 100 µM nitrate instead of 882 µM) (Fig. 1). In chemostat cultures, cell concentrations are controlled by the nitrogen concentration of the medium (100 µM) and the growth rate is controlled by the dilution rate. Slow-growing nutrient-limited prey were maintained at a specific growth rate of 0.2 d^{-1}, and fast-growing nutrient-limited prey were maintained at 1.2 d^{-1} according to the equation:

$$\mu = F/V \quad (1)$$

where µ is specific growth rate (d^{-1}), F is the flow rate (l d^{-1}) of medium into and out of the culture vessel, and V is culture volume (l). This range of phytoplankton growth rates was considerably wider than previous work using prey in steady-state nutrient-limited growth (Golz et al. 2015), and therefore yielded a wider range of prey C:N and carbon compositions (Halsey et al. 2010, 2011). Filtered air was constantly pumped into the culture vessel to maintain sufficient CO_2 availability and to keep cells evenly suspended. Once the phytoplankton prey reached steady-state growth (defined as population and chlorophyll changes <5% over 3 to 7 d), *O. marina* were introduced from a stock culture into the second stage of the 2-stage continuous culture system (0.3 l) at an initial concentration of 10^3 cells ml^{-1}. Prey culture from Stage 1 was pumped directly into the second stage at a constant rate of 60 ml d^{-1} with outflow also kept constant at 60 ml d^{-1} (Fig. 1). Thus, once in steady-state, the growth rate of *O. marina* in Stage 2 was kept constant between treatments at 0.2 d^{-1}. This experimental design allowed us to constrain the amount of prey carbon delivered to Stage 2 between *O. marina* treatments (see Table 1) while varying prey carbon composition (by altering their nutrient-limited growth rates). The *O. marina* growth rate of 0.2 d^{-1} is lower than reported maximal growth rates but is well within the range of those reported for *O. marina* grown on a range of different prey (see, for example, Goldman et al. 1989, Apple et al. 2011, Yang et al. 2013). The Stage 2 culture that contained *O. marina* was wrapped in foil to minimize light and prevent growth of the prey. Experimental measurements (see below) were initiated when *O. marina* in Stage 2 reached steady-state growth as defined by population changes <5% over 3 to 7 d. All experimental measurements of predator and prey physiology were done in triplicate and staggered over a 3 wk period to avoid sampling >10% of culture volume on any single day. This schedule allowed all cultures of prey and *O. marina* to remain in steady-state growth throughout each independent experiment.

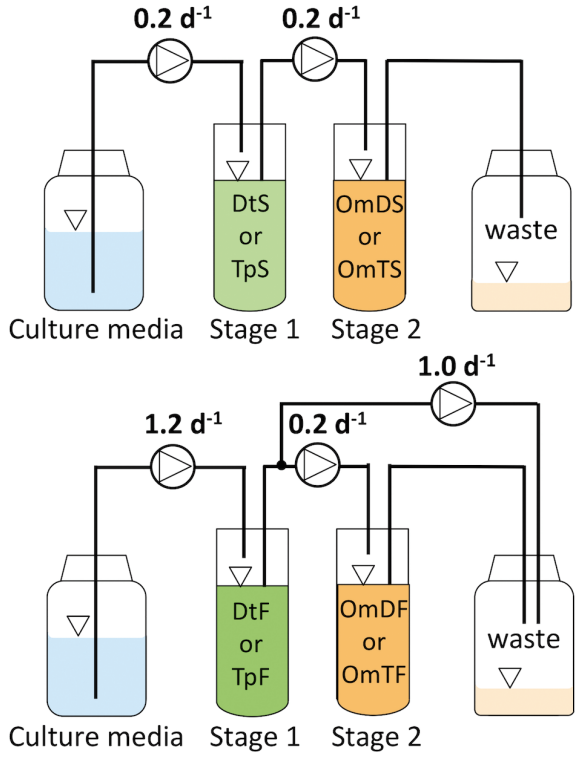

Fig. 1. Two-stage continuous culture used in this study to investigate the influence of growth rate-dependent changes in prey carbon composition on *Oxyrrhis marina* physiology. Culture medium was pumped into Stage 1 containing either *Dunaliella tertiolecta* or *Thalassiosira pseudonana*. The steady-state nutrient-limited growth rate of the prey was either 0.2 d^{-1} (top) or 1.2 d^{-1} (bottom). In all treatments, prey were fed to *O. marina* such that grazers maintained a constant growth rate of 0.2 d^{-1}. Not shown are filtered air and sampling ports into each stage. DtS: slow-growing *D. tertiolecta*; TpS: slow-growing *T. pseudonana*; DtF: fast-growing *D. tertiolecta*; TpF: fast-growing *T. pseudonana*. See Table 1 for abbreviations for *O. marina* treatments

Both phytoplankton cultures in Stage 1 were maintained axenically as determined by microscopy and plating onto marine broth agar plates. *O. marina* obtained from NCMA was not axenic. We used microscopy and dilution plating onto marine broth agar plates to confirm that bacterial counts did not increase throughout the experiments and did not vary between *O. marina* treatments. Nevertheless, bacterial remineralization of organic matter could increase nitrogen concentrations in Stage 2. It is also possible that prey entering Stage 2 were temporarily exposed to higher nitrogen concentrations due to remineralization of prey and/or bacterial biomass by *O. marina*. Sudden exposure of the N-limited prey to increased

nitrogen concentrations could cause them to rapidly assimilate N. However, such shifts in N-status would dampen any treatment effects measured in *O. marina* in this study. Therefore, the significant differences between *O. marina* treatments reported in this study can be attributed to the nutrient-limited, growth-rate-dependent changes in prey composition and not to assimilation of remineralized N. Triplicate independent 2-stage continuous cultures were established for each nutrient-limited growth rate and prey species. Thus, in total, 12 two-stage continuous cultures were established and sampled for this study (2 prey types × 2 nutrient-limited growth rates × 3 replicates).

Experimental measurements

Cell densities and volumes were monitored using a Coulter Counter (Beckman Coulter). Particulate carbon and nitrogen content were determined by filtering 2, 3, and 4 ml of prey cultures (Stage 1) or 3, 4, and 5 ml of *O. marina* cultures (Stage 2) onto pre-combusted GF/F filters to verify linear relationships between C or N and volume filtered. Culture filtrate (4 ml) was also filtered through a pre-combusted GF/F filter and used for blank subtraction. Filters were stored at −20°C until elemental analysis (Exeter Analytical). In this study, we refer to 'particulates' as the material in Stage 2 collected on the GF/F filter, which includes *O. marina* cells and fecal pellets. To determine the non-prey elemental contents of particulates in Stage 2 (*O. marina* biomass plus fecal pellets), the elemental contents of the residual prey in Stage 2 were subtracted from the total elemental contents in Stage 2 (in µg C or N ml^{-1}) according to the equation:

$$E_g = [\text{Stage 2 C or N} - (C_p \times P_2)] \quad (2)$$

where E_g is non-prey particulate carbon or nitrogen concentration in Stage 2 (in µg C or N ml^{-1}), C_p is prey carbon or nitrogen content in Stage 1 (in µg C or N $cell^{-1}$), and P_2 is the prey population (in cells ml^{-1}) in Stage 2.

Phosphorus contents were determined by filtering 5 ml of culture onto an acid-washed and pre-combusted GF/F filter. Culture filtrate was filtered through another prepared GF/F filter and used for blank-subtraction. Phosphorus content was determined following the established protocol described in (Valderrama 1981) using standards prepared with KH_2PO_4. Chlorophyll concentration was measured to monitor nutritional status and acclimation status of the phytoplankton cells in Stage 1. Chlorophyll was below detection in Stage 2. Chlorophyll content was determined by gently filtering cultures through a GF/F filter and extracting in 90% acetone at −20°C for 24 to 48 h. Absorbance was measured by spectrophotometer (Shimadzu) and calculated using established extinction coefficients for chlorophytes and diatoms (Ritchie 2006).

CTEs or NTEs quantify the fraction of prey carbon or nitrogen consumed and retained in *O. marina* particulate matter (i.e. *O. marina* biomass and fecal pellets). CTE and NTE were calculated by dividing *O. marina* particulate elemental content by the amount of prey elemental content that was consumed using the following equation:

$$\frac{E_g}{C_p(P_1 - P_2)} \quad (3)$$

where E_g, C_p, and P_2 are described above, and P_1 is the prey population (in cells ml^{-1}) in Stage 1.

Ingestion rates that accounted for the constant dilution of Stage 2 were calculated using the following equation (Bloem et al. 1988):

$$\mu \times \frac{P_1 - P_2}{G} \quad (4)$$

where µ is the specific growth rate in Stage 2 (also the specific dilution rate, d^{-1}) and G is the predator population in cells ml^{-1}.

DOC content in Stage 2 was measured to help determine the fates of prey carbon in the different *O. marina* treatments. A 5 ml sample of Stage 2 culture was gently filtered on a pre-combusted GF/F filter and collected in a combusted vial. The sample was then acidified with 1 N HCl by addition of 4% of the sample volume. Sample blanks were generated the same way but with sterile f/2 medium. All samples were analyzed using a Shimadzu Total Organic Carbon (TOC) analyzer.

Neutral lipid content in the prey and their *O. marina* predators were visualized using Nile Red and confocal microscopy. Samples (1 ml) were incubated in the dark for 4 h with Nile Red dye (0.001 g per 10 ml acetone) prior to imaging using an Argon laser (458, 488, 514 nm) at 63× magnification on a LSM 780 NLO confocal microscope (Zeiss). Neutral lipids were detected by emission at 575 nm and chlorophyll autofluorescence was detected at 700 nm.

RESULTS

Two-stage continuous cultures were established to study how differences in phytoplankton carbon composition influenced its allocation in *Oxyrrhis*

marina. Cell properties including C:Chl and C:N of the prey species *Dunaliella tertiolecta* and *Thalassiosira pseudonana* increased with decreasing growth rates and were similar to values previously reported for these species growing under steady-state nutrient-limited conditions (Table 1) (Eppley & Renger 1974, Laws & Bannister 1980, Halsey et al. 2010). Prey concentrations in Stage 2 were approximately one-tenth their concentrations in Stage 1. The rate of prey carbon delivery from Stage 1 to *O. marina* in Stage 2 was 1 to 2 mg C d^{-1} in all treatments (Table 1).

O. marina cell densities in Stage 2 of the continuous culture system were 1.9 to 2.6 × 10^4 cells ml^{-1}, depending on the treatment (Table 1). Hereafter, *O. marina* growing on slow- or fast-growing *D. tertiolecta* are referred to as OmDS and OmDF, respectively, and *O. marina* growing on slow- or fast-growing *T. pseudonana* are referred to as OmTS and OmTF, respectively. Cellular ingestion rates (prey cells [*O. marina*] d^{-1}) of OmDF were 1.6-fold higher than OmDS, but cellular ingestion rates of OmTF were not significantly different than OmTS (Table 1). However, when the cellular ingestion rates were converted to prey carbon consumed, the carbon ingestion rate of OmTS was 1.3 to 1.7-fold higher than all other *O. marina* treatments (Table 1).

CTEs in *O. marina* fed either *D. tertiolecta* or *T. pseudonana* were strongly impacted by the growth rate of their prey. CTE was 43 ± 15% (SD) in OmDF and declined to 17 ± 6% in OmDS (Fig. 2A). CTE was 27 ± 5% in OmTF and decreased to only 3 ± 2% in OmTS (Fig. 2A). CTEs were also strongly influenced by prey species; CTEs in OmDF and OmDS were 1.4 and 4.9-fold higher than the CTEs in OmTF and OmTS, respectively. In contrast, NTEs were similar across all *O. marina* treatments (Fig. 2B).

The remarkable differences in CTEs between *O. marina* fed different nutrient-limited prey led us to ask how the fates of prey carbon consumed by the microzooplankton varied between treatments. In addition to assimilation into *O. marina* particulates (biomass and fecal pellets), prey carbon may be excreted into the medium as DOC or respired back to CO_2. DOC was significantly higher in Stage 2 when *O. marina* was fed *D. tertiolecta* compared to *O. marina* fed *T. pseudonana*, but prey growth rate did not influence DOC concentrations in Stage 2 (Fig. 3). Thus, we conclude that the vast majority of *T. pseudonana* carbon was remineralized to CO_2.

The elemental stoichiometry of *O. marina* fed *D. tertiolecta* did not vary in response to the growth rate of the prey. However, C:N and C:P in OmTS were significantly lower than OmDF (p = 0.01 and 0.048,

Table 1. Characteristics of cultures growing in the 2-stage chemostat system. Stage 1 contained either *Dunaliella tertiolecta* or *Thalassiosira pseudonana* prey growing at specific growth rates of 0.2 or 1.2 d^{-1}. Prey from Stage 1 flowed to *Oxyrrhis marina* in Stage 2 at a rate of 60 ml d^{-1} and resulted in a similar amount of prey carbon supplied to *O. marina* between treatments. Values in parentheses: SD of 3 independent 2-stage continuous cultures. Variances shown in *italics* were determined by propagation of uncertainty. OmDS: *O. marina* fed slow-growing *D. tertiolecta*; OmTS: *O. marina* fed slow-growing *T. pseudonana*; OmDF: *O. marina* fed fast-growing *D. tertiolecta*; OmTF: *O. marina* fed fast-growing *T. pseudonana*

	D. tertiolecta		*T. pseudonana*	
Stage 1				
Growth rate (d^{-1})	0.2	1.2	0.2	1.2
Cell density (cells ml^{-1})	4.96 × 10^5 (2.47×10^4)	7.69 × 10^5 (5.30×10^4)	1.99 × 10^6 (3.09×10^5)	1.69 × 10^6 (2.75×10^5)
Cell volume (μm^3)	180 (21)	119 (8)	33 (3)	37 (3)
C:Chl ($\mu g\ \mu g^{-1}$)	238 (*70*)	59 (*10*)	514 (*109*)	125 (*16*)
C:N	14.0 (*3.3*)	5.5 (*1.2*)	11.4 (*2.8*)	7.1 (*1.1*)
C concentration ($\mu g\ ml^{-1}$)	23.3 (1.1)	16.7 (2.0)	35.0 (4.1)	16.3 (1.5)
Rate of prey carbon flow into Stage 2 (mg C d^{-1})	1.40 (0.06)	1.00 (0.12)	2.10 (0.25)	0.98 (0.09)
Stage 2				
Abbreviation for *O. marina* treatment	OmDS	OmDF	OmTS	OmTF
Prey cell density (cells ml^{-1})	3.54 × 10^4 (2.10×10^3)	1.85 × 10^4 (2.17×10^3)	2.22 × 10^5 (1.33×10^5)	1.97 × 10^5 (1.92×10^4)
O. marina cell density (cells ml^{-1})	2.36 × 10^4 (4.32×10^3)	2.33 × 10^4 (4.73×10^3)	2.59 × 10^4 (5.34×10^3)	1.90 × 10^4 (4.41×10^3)
O. marina cell volume (μm^3)	1970 (198)	1729 (144)	1382 (140)	1467 (248)
O. marina C concentration ($\mu g\ ml^{-1}$)	4.0 (0.21)	7.0 (0.49)	1.2 (0.03)	4.5 (0.20)
Prey ingestion rate (prey cells [*O. marina*] d^{-1})	3.90 (*0.77*)	6.44 (*1.44*)	13.79 (*8.91*)	15.71 (*4.71*)
Prey carbon ingestion rate (ng C [*O. marina*] d^{-1})	0.184 (*0.016*)	0.140 (*0.020*)	0.240 (*0.048*)	0.152 (*0.028*)

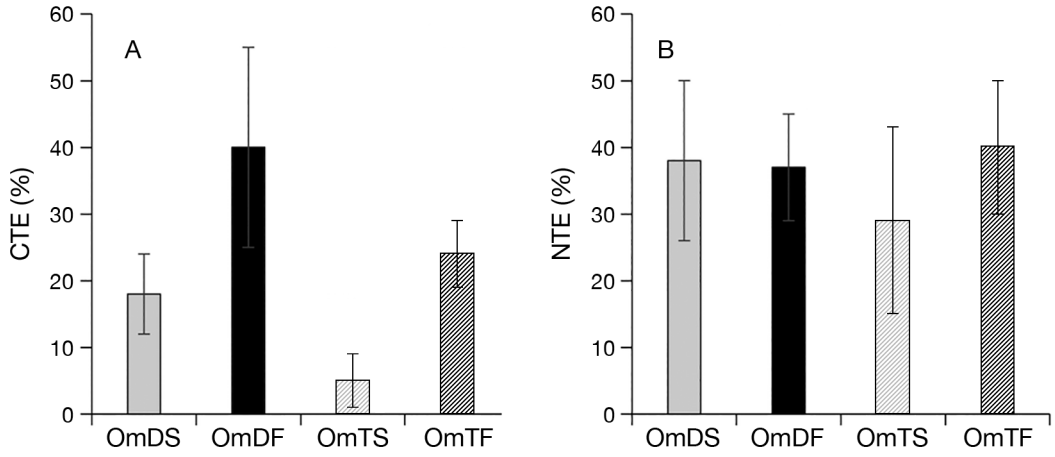

Fig. 2. Carbon transfer efficiencies (CTEs) and nitrogen transfer efficiencies (NTEs) in *Oxyrrhis marina* fed *Dunaliella tertiolecta* (filled bars) and *O. marina* fed *Thalassiosira pseudonana* (hatched bars); *O. marina* fed slow-growing prey (grey); *O. marina* fed fast-growing prey (black). Errors bars: variances determined by propagation of uncertainty. See Table 1 for culture definitions

respectively, *t*-test; Table 2, Fig. 4). Overall, OmTS maintained a higher proportion of cellular nitrogen and phosphorus compared to *O. marina* fed any of the other prey.

The influence of growth-rate-dependent differences in phytoplankton prey on *O. marina* physiology was also studied using Nile Red staining and confocal microscopy to visualize neutral-lipid body accumulation. First, neutral-lipid body accumulation in the different phytoplankton prey was observed (Fig. 5A). In fast-growing *D. tertiolecta*, lipid bodies (~1 µm in diameter) were visible in all of the cells imaged. In contrast, lipid bodies were rarely visible

Table 2. Elemental composition of *Oxyrrhis marina* grown on slow- or fast-growing nutrient-limited *Dunaliella tertiolecta* or *Thalassiosira pseudonana.* See Table 1 for *O. marina* treatment abbreviations. Values in parentheses are variances determined by propagation of uncertainty using data from 3 independent 2-stage continuous cultures

O. marina treatment	C:N		N:P		C:P	
	Molar ratio	Mass ratio	Molar ratio	Mass ratio	Molar ratio	Mass ratio
OmDS	6 (1)	5 (1)	8 (3)	4 (1)	39 (22)	15 (9)
OmDF	6 (3)	5 (1)	8 (3)	4 (1)	41 (20)	16 (8)
OmTS	3 (1)	3 (1)	5 (3)	2 (2)	11 (9)	4 (3)
OmTF	5 (2)	4 (2)	7 (4)	3 (2)	34 (14)	13 (5)

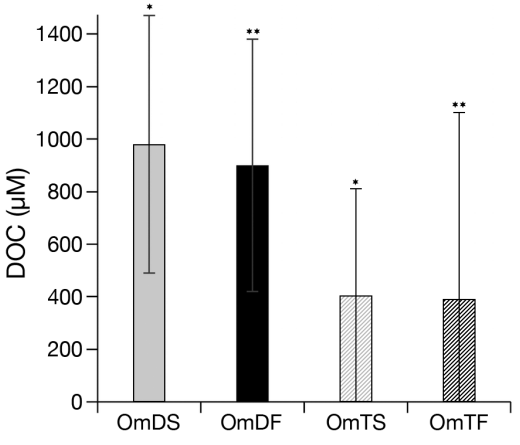

Fig. 3. Dissolved organic carbon (DOC) in Stage 2 of the 2-stage continuous culture system. *Oxyrrhis marina* fed *Dunaliella tertiolecta* (filled bars); *O. marina* fed *Thalassiosira pseudonana* (hatched bars); *O. marina* fed slow-growing prey (grey); *O. marina* fed fast-growing prey (black). Error bars: SD of 3 independent replicates. Treatments with the same symbols were significantly different (*p = 0.0002; **p = 0.002; independent samples *t*-test). See Table 1 for culture definitions

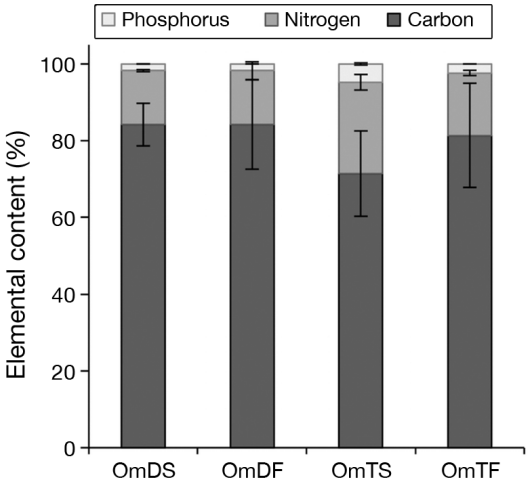

Fig. 4. Cellular elemental composition by mass of *Oxyrrhis marina* fed slow- or fast-growing *Dunaliella tertiolecta* or *Thalassiosira pseudonana.* Carbon (dark grey), nitrogen (medium grey), phosphorus (light grey). Error bars: variances determined by propagation of uncertainty. See Table 1 for culture definitions

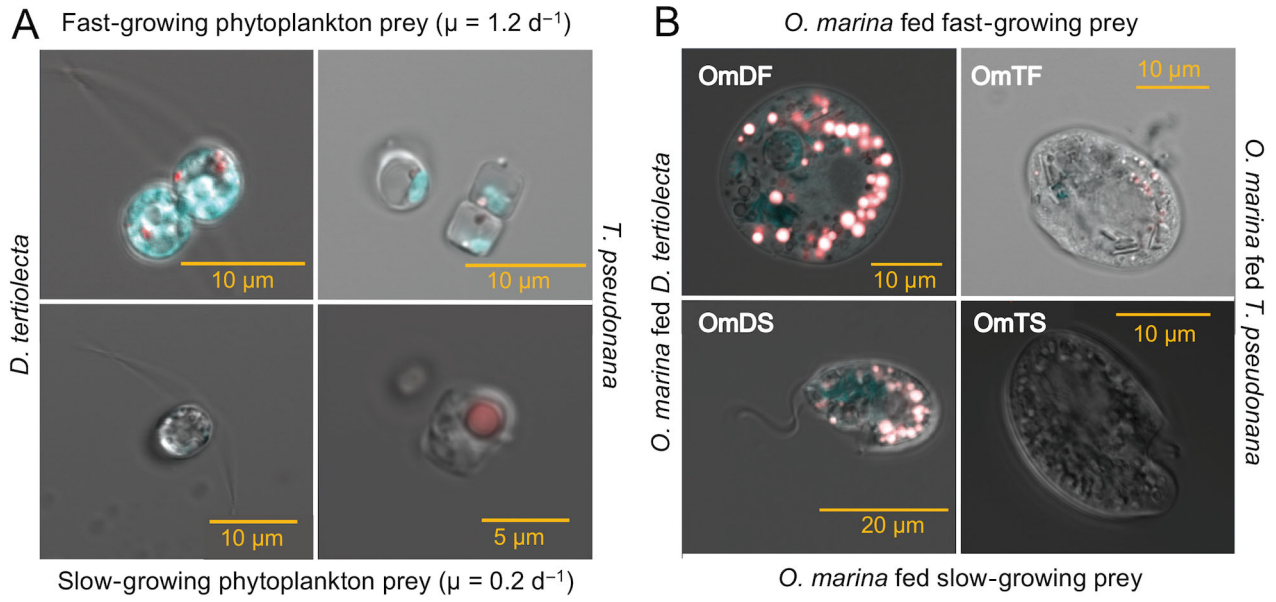

Fig. 5. Neutral-lipid body accumulation in (A) nutrient-limited prey species and (B) their *Oxyrrhis marina* predators. Confocal images of typical cells showing Nile Red-stained lipid bodies (red) in fast-growing prey and OmDF and OmTF (top row; see Table 1 for culture definitions) or slow-growing prey and OmDS and OmTS (bottom row). Green: chlorophyll autofluorescence. For each species and treatment, at least 30 cells were imaged and are representative of at least 90 to 150 cell observations

in slow-growing *D. tertiolecta* cells. Lipid bodies that were ~0.5 µm in diameter were observed in the majority of the fast-growing *T. pseudonana* imaged. However, slow-growing *T. pseudonana* cells displayed either single lipid bodies (~2 µm in diameter) that encompassed approximately 25% of total cell volume (Fig. 5A) or multiple, smaller lipid bodies.

O. marina neutral-lipid body accumulation was markedly different depending on prey species (Fig. 5B). The growth rate of *D. tertiolecta* did not appear to influence *O. marina* lipid body accumulation. Regardless of whether *O. marina* was fed fast- or slow-growing *D. tertiolecta*, *O. marina* accumulated multiple ~2 µm diameter lipid bodies in the majority of imaged cells (Fig. 5B). In contrast, OmTF accumulated very few <1 µm diameter lipid bodies, and OmTS showed no visible lipid bodies (Fig. 5B).

DISCUSSION

We used 2-stage continuous cultures to control phytoplankton carbon composition and examine the fate of prey carbon into microzooplankton particulates, DOC, and CO_2. This culturing system ensured that the amount of prey carbon provided to *Oxyrrhis marina* was constrained between treatments but prey composition varied with nutrient-limited growth rate (Halsey et al. 2011, Halsey & Jones 2015). This approach was motivated by the idea that microzooplankton sometimes have a steady supply of prey that are acclimated to nutrient-limitation, such as during months of strong seasonal stratification. In all treatments, *O. marina* maintained stable populations and constant, positive growth rates for at least 3 wk. Carbon ingestion rates were less than the maximal ingestion rates reported for *O. marina* grown on green algae (Roberts et al. 2011), as would be expected in the conditions of a chemostat. Yet, in all treatments, *O. marina* cell volumes were similar to carbon-replete *O. marina* cells and larger than starved *O. marina* cells (Pelegrí et al. 1999, Anderson & Menden-Deuer 2017). Furthermore, prey cells were never fully depleted from the *O. marina* culture, maintaining a ratio of about 1:1 *O. marina*:prey cells. These observations support the conclusion that the 2-stage continuous culture system was effective for studying the responses of growing, carbon-limited but non-starving microzooplankton cells to prey that varied in growth rate.

CTEs in *O. marina* fed slow-growing nutrient-limited prey were 60 to 89% lower than CTEs in *O. marina* fed the faster-growing prey (Fig. 2A). Prey species compounded the effect of growth rate, with the CTEs in *O. marina* fed *Thalassiosira pseudonana* being consistently lower than *O. marina* fed *Dunaliella tertiolecta*. These differences in CTEs were not due to differences in the rates of prey carbon fed to *O. marina*, because OmTS consumed more prey carbon than any of the other *O. marina* treatments (Table 1) yet retained only 3.3% of consumed prey

carbon in particulate matter (*O. marina* biomass and fecal material). Besides having the lowest CTE, OmTS also had the smallest cell volume (1382 μm^3), while OmDF had the highest CTE and largest cell volume (1970 μm^3). Finally, the low CTE in OmTS was not associated with higher DOC content in Stage 2 compared to OmTF. Thus, we can infer that in OmTS, the vast majority of ingested diatom carbon was lost from the system as CO_2 instead of being packaged into particulate carbon (*O. marina* biomass and fecal pellets) or excreted as DOC (Mitra 2006, Meunier 2012). Slow-growing, nutrient-limited *T. pseudonana* narrowly supported a diet sufficient for steady-state growth. On the other hand, fast-growing algae appear to promote greater carbon transfer to higher trophic levels and export from the euphotic zone. The consequence of low CTEs in microzooplankton is an abridged marine carbon cycle that limits carbon export and the larger food web via the biological carbon pump.

The impacts of prey nutritional status on CTEs reported in this study confirm a form of stoichiometric modulation of predation (SMP; Mitra & Flynn 2005) in which poor prey quality causes higher rates of prey ingestion that are insufficient to overcome lower assimilation efficiencies (Mitra et al. 2007). Although these SMP dynamics were observed in batch cultures of copepods (Jones & Flynn 2005), they were not expected to be displayed by microzooplankton (Mitra 2006). The results reported for OmTS provide strong evidence for this form of SMP in *O. marina*.

O. marina maintained elemental homeostasis with a balanced C:N:P of 48:8:1 in all treatments except for OmTS. In that treatment, C:N:P was 15:5:1, reflecting that *O. marina* cells were severely depleted in carbon relative to nitrogen and phosphorus. C:N in OmTS was even lower than in *O. marina* following 4 d diets of N-starved algae (Hantzsche & Boersma 2010, Meunier 2012). This exceptionally low elemental ratio was probably revealed by use of the 2-stage chemostat system that facilitated steady-state growth in both the prey and microzooplankton. These growth conditions are markedly different than the short-term starvation experiments more commonly conducted for microzooplankton studies. Microbial physiology is highly sensitive to environmental acclimation. The differences in phytoplankton responses to steady-state nutrient limitation compared to starvation have been discussed in the literature (MacIntyre & Cullen 2005, Halsey & Jones 2015). Clearly, microzooplankton physiology also varies depending on whether they are (1) consuming prey that are in balanced (or steady-state) growth or starved, and (2) provided a constant or pulsed dietary regime (Roberts et al. 2011, Anderson & Menden-Deuer 2017, this study).

The exceptionally low C:N:P in OmTS compared to the other treatments suggests that OmTS obtained sufficient nitrogen and phosphorus to serve cell functions and maintain steady-state growth but rapidly respired prey carbon for energetic requirements (Hantzsche & Boersma 2010, Meunier 2012) and/or to metabolize prey carbon for biosynthesis of essential carbon compounds not obtained directly from slow-growing *T. pseudonana* (Hessen & Anderson 2008). Although C:N values of 3 have been measured in marine microalgae (Geider & La Roche 2002), to our knowledge such low values have not been previously reported in microzooplankton. Cells growing at the edge of their resource requirements (e.g. OmTS) are expected to conserve protein and nucleic acids but deplete reserves of carbohydrate and lipid (Morris 1980, Halsey et al. 2011, Halsey & Jones 2015). The C:N ratio of average protein is 3.2 (Russell-Hunter 1970). Under N-limitation, ~85% of nitrogen in microalgae is allocated to protein, which can account for up to 65% of cell mass (Morris 1980, Laws 1991, Lourenco et al. 1998). The C:N of nucleic acids is 2.6, and RNA can account for up to 14% of microalgal cell mass (Geider & LaRoche 2002). Finally, nitrogenous osmolytes can be significant contributors to cell nitrogen, but osmolyte content appears to be highly variable depending on species and nutrient-limited growth rate (Keller et al. 1999). Thus, these 3 carbon pools are likely to underlie the low C:N measured in OmTS.

NTEs were ≥CTEs in all *O. marina* treatments. NTEs < CTEs were reported in starving or dying copepods that had been fed a diet composed only of nutrient-replete diatoms; however, the relationship reversed so that NTE ≥ CTE in copepods whose diatom diets were supplemented with dinoflagellates (Jones & Flynn 2005). All of the *O. marina* treatments in our study maintained stable growth despite being fed mono-species diets, albeit with widely varying CTEs, even when *D. tertiolecta* or *T. pseudonana* were severely N-limited.

The lower CTEs in *O. marina* when fed diatoms compared to green algae may reflect high energetic costs associated with extracting cell biomass from the silica frustules surrounding diatoms. Diatom frustule morphology provides protection from grazing (Hamm et al. 2003), and iron limitation increases frustule mechanical strength (Wilken et al. 2011) due to longer periods of silica deposition during cell cycle arrest. Such frustule strengthening may also occur during macronutrient (N or P) limitation (Claquin et

al. 2002). Thus, high rates of respiration may be required to fuel the additional ATP requirements needed for consumption of diatoms, and especially severely N-limited diatoms (e.g. *T. pseudonana* growing at only 0.2 d^{-1}). Consumption of green algae, on the other hand, may be inherently less costly to consume due to the lack of a silica barrier.

Microzooplankton lipids have emerged as critical prey components for the development of their larger grazers; for example, in copepod, crab, and fish larvae development (Sulkin & McKeen 1999, Frost et al. 2005, Klein Breteler et al. 2005). Many marine heterotrophs obtain essential fatty acids or fatty acid precursors from their diet, and *O. marina* can apparently synthesize essential fatty acids from simple sources of organic carbon (i.e. acetate; Lund et al. 2008). The differences in lipid body accumulation in green algae and diatoms (Fig. 5A) provided us the opportunity to examine whether these differences in prey carbon composition were related to CTE in *O. marina*.

Neutral lipid accumulation varied substantially between *O. marina* treatments. Nile Red does not distinguish between neutral lipid types (e.g. α-linolenic acid [ALA], eicosapentaenoic acid [EPA], or docosahexaenoic acid [DHA]), but the process of lipid metabolism shown in Fig. 6 suggests how *O. marina* likely utilizes the lipids available in their prey (Bergé & Barnathan 2005). *O. marina* fed *D. tertiolecta* were rich in neutral-lipid bodies. Some of the neutral-lipid bodies in *O. marina* may have been obtained directly from *D. tertiolecta*, but this is unlikely because lipid bodies were not detected in *O. marina* digestion vacuoles. Neutral lipids could also have been produced de novo from DOC in the system (Lund et al. 2008). However, the high lipid-body content in OmDF and OmDS suggests that the bulk of *O. marina* lipid bodies were derived from phospholipids that are enriched in *D. tertiolecta* (Halsey et al. 2011).

Even though neutral-lipid body content appeared to be greatest in slow-growing *T. pseudonana*, *O. marina* fed either fast or slow-growing *T. pseudonana* lacked the conspicuous lipid bodies found in *O. marina* fed *D. tertiolecta*. The marginal CTE in OmTS suggested that there was nearly no excess energy available in the slow-growing *T. pseudonana* carbon to enable lipid body storage in *O. marina*. Because slower-growing photoautotrophic cells typically have lower phospholipid content than faster growing cells (Halsey et al. 2011, Meï et al. 2015), we hypothesize that slow-growing *T. pseudonana* were low in phospholipid content and had already oxidized EPA to DHA to obtain energy in the form of NADH for growth (Fig. 6). Thus, despite the fact that their prey

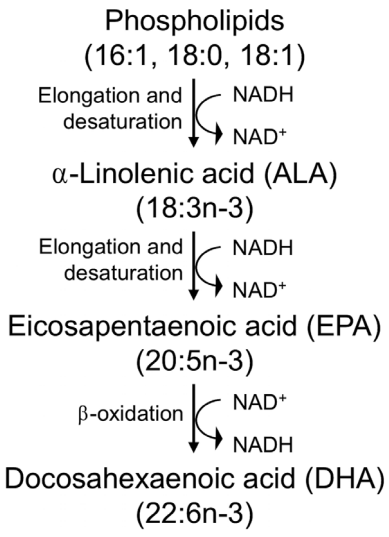

Fig. 6. Expected pathway for polyunsaturated fatty acid synthesis in *Oxyrrhis marina*. Synthesis of EPA requires inputs of reductant in the form of NADH, but cells can regenerate NADH from EPA by conversion to DHA (Bergé & Barnathan 2005)

accumulated a large pool of neutral lipids, OmTS oxidized those prey lipids back to CO_2 or salvaged that prey carbon for metabolic needs instead of retaining them in neutral-lipid bodies or biomass.

The lack of neutral-lipid bodies observed in OmTS and OmTF also suggests that microzooplankton feeding on nutrient-limited diatoms will negatively impact growth and fitness of organisms at higher trophic levels (Kiørboe 1989, Sulkin & McKeen 1999, Montagnes et al. 2011). Neutral lipid (long-chain fatty acid) characterization of our prey and *O. marina* treatments is needed to confirm the prey-influenced lipid metabolism processes proposed above for *O. marina* (Anderson & Pond 2000, Anderson et al. 2004). Nevertheless, this work demonstrates that microzooplankton are not homeostatic with respect to their lipid content, contradicting assumptions upon which ecosystem models describing trophic and elemental transfers are based (Anderson et al. 2013).

CONCLUSIONS

Growth-rate-dependent carbon composition strongly altered the fate of carbon consumed by the model microzooplankter *Oxyrrhis marina*. There appears to be a hierarchy of prey quality with fast-growing prey providing the most beneficial *O. marina* diet as reflected by higher CTEs and neutral lipid accumulation. In contrast, slower-growing prey yielded lower CTEs, and in the case of *Thalassiosira pseudonana*,

an *O. marina* population that retained virtually no neutral lipid bodies. Even though OmTS maintained steady-state growth, these microzooplankton would be unlikely to provide essential fatty acids for macrozooplankton growth and development. Thus, slow-growing diatom prey could significantly abbreviate the microbial food web.

The dramatic impacts of nutrient-limited phytoplankton growth rates on carbon allocation in microzooplankton give insight into how changing ocean conditions and community structure will impact food-web dynamics and carbon cycling. These controlled experiments demonstrate the physiological capacity for microzooplankton to grow in very low-nutrient environments, but our experimental design revealed a greater range of microzooplankton physiological flexibility than is currently captured in marine ecosystem models. Whether microzooplankton respond in the same manner to phytoplankton growing under different types of resource-limited growth rates (e.g. light, trace metals, phosphorus), as was observed for nutrient-limited growth rates, is an outstanding question that should be addressed to develop a comprehensive understanding of the immediate fates of primary production.

Acknowledgements. The authors thank Elizabeth Harvey and the anonymous reviewers of this manuscript whose questions and comments greatly improved the final version.

LITERATURE CITED

Andersen T, Færøvig PJ, Hessen DO (2007) Zooplankton carrying capacity as related to quality and quantity of food. Limnol Oceanogr 52:2128–2134

Anderson SR, Menden-Deuer S (2017) Growth, grazing, and starvation survival in three heterotrophic dinoflagellate species. J Eukaryot Microbiol 64:213–225

Anderson TR, Pond DW (2000) Stoichiometric theory extended to micronutrients: comparison of the roles of essential fatty acids, carbon, and nitrogen in the nutrition of marine copepods. Limnol Oceanogr 45:1162–1167

Anderson TR, Boersma M, Raubenheimer D (2004) Stoichiometry: linking elements to biochemicals. Ecology 85: 1193–1202

Anderson TR, Hesson DO, Mitra A, Mayor DJ (2013) Sensitivity of predicted secondary production and export flux to choice of trophic transfer formulation in marine ecosystem models. J Mar Syst 125:41–53

Apple JK, Strom SL, Palenik B, Brahamsha B (2011) Variability in protist grazing and growth on different marine *Synechococcus* isolates. Appl Environ Microbiol 77: 3074–3084

Bergé JP, Barnathan G (2005) Fatty acids from lipids of marine organisms: molecular biodiversity, roles as biomarkers, biologically active compounds and economical aspects. Adv Biochem Eng Biotechnol 96:49–125

Bi R, Arndt C, Sommer U (2014) Linking elements to biochemicals: effects of nutrient supply ratios and growth rates on fatty acid composition of phytoplankton species. J Phycol 50:117–130

Bloem J, Starink M, Bär-Gilissen MJB, Cappenberg TE (1988) Protozoan grazing, bacterial activity, and mineralization in two-stage continuous cultures. Appl Environ Microbiol 54:3113–3121

Bull AT (2010) The renaissance of continuous culture in the post-genomics age. J Ind Microbiol Biotechnol 37: 993–1021

Calbet A, Landry MR (2004) Phytoplankton growth, microzooplankton grazing, and carbon cycling in marine systems. Limnol Oceanogr 49:51–57

Caron DA, Hutchins DA (2013) The effects of changing climate on microzooplankton grazing and community structure: drivers, predictions and knowledge gaps. J Plankton Res 35:235–252

Chalup MS, Laws EA (1990) A test of the assumptions and predictions of recent microalgal growth models with the marine phytoplankter *Pavlova lutheri*. Limnol Oceanogr 35:583–596

Chu FLE, Lund ED, Podbesek JA (2008) Quantitative significance of n-3 essential fatty acid contribution by heterotrophic protists in marine pelagic food webs. Mar Ecol Prog Ser 354:85–95

Chu FLE, Lund ED, Littreal PR, Ruck KE, Harvey E (2009) Species-specific differences in long-chain n-3 essential fatty acid, sterol, and steroidal ketone production in six heterotrophic protist species. Aquat Biol 6:159–172

Claquin P, Martin-Jezequel V, Kromkamp JC, Veldhuis MJW, Kraay GW (2002) Uncoupling of silicon compared with carbon and nitrogen metabolims and the role of the cell cycle in continuous cultures of *Thalassiosira pseudonana* (Bacillariophyceae) under light, nitrogen, and phosphorus control. J Phycol 38:922–930

Cullen JJ, Yang X, MacIntyre HL (1992) Nutrient limitation of marine photosynthesis. In: Falkowski PG, Woodhead AD (eds) Primary productivity and biogeochemical cycles in the sea. Plenum Press, New York, NY, p 69–88

Curds CR, Cockburn A (1971) Continuous monoxenic culture of *Tetrahymena pyriformis*. J Gen Microbiol 66:95–108

Darchambeau F, Faer vig PJ, Hessen DO (2003) How *Daphnia* copes with excess carbon in its food. Oecologia 136: 336–346

Eppley RW, Renger EH (1974) Nitrogen assimilation of an oceanic diatom in nitrogen-limited continuous culture. J Phycol 10:15–23

Frost PC, Evans-White MA, Finkel ZV, Jensen TC, Matzek V (2005) Are you what you eat? Physiological constraints on organismal stoichiometry in an elementally imbalanced world. Oikos 109:18–28

Geider RJ, La Roche J (2002) Redfield revisited: variability of C:N:P in marine microalgae and its biochemical basis. Eur J Phycol 37:1–17

Goldman JC, Dennett MR, Gordin H (1989) Dynamics of herbivorous grazing by the heterotrophic dinoflagellate *Oxyrrhis marina*. J Plankton Res 11:391–407

Golz AL, Burian A, Winder M (2015) Stoichiometric regulation in micro- and mesozooplankton. J Plankton Res 37: 293–305

Guillard RRL (1975) Culture of phytoplankton for feeding marine invertebrates. In: Smith WL, Chanley MH (eds) Culture of marine invertebrate animals. Plenum Press, New York, NY, p 29–60

Halsey KH, Jones BM (2015) Phytoplankton strategies for photosynthetic energy allocation. Annu Rev Mar Sci 7: 265–297

Halsey KH, Milligan AJ, Behrenfeld MJ (2010) Physiological optimization underlies growth rate-independent chlorophyll-specific gross and net primary production. Photosynth Res 103:125–137

Halsey KH, Milligan AJ, Behrenfeld MJ (2011) Linking time-dependent carbon-fixation efficiencies in *Dunaliella tertiolecta* (Chlorophyceae) to underlying metabolic pathways. J Phycol 47:66–76

Halsey KH, O'Malley RT, Graff JR, Milligan AJ, Behrenfeld MJ (2013) A common partitioning strategy for photosynthetic products in evolutionarily distinct phytoplankton species. New Phytol 198:1030–1038

Halsey KH, Milligan AJ, Behrenfeld MJ (2014) Contrasting strategies of photosynthetic energy utilization drive lifestyle strategies in ecologically important picoeukaryotes. Metabolites 4:260–280

Hamm CE, Merkel R, Springer O, Poitr J, Maier C, Prechtel K, Smetacek V (2003) Architecture and material properties of diatom shells provide effective mechanical protection. Nature 421:841–843

Hantzsche FM, Boersma M (2010) Dietary-induced responses in the phagotrophic flagellate *Oxyrrhis marina.* Mar Biol 157:1641–1651

Herzig R, Falkowski PG (1989) Nitrogen limitation in *Isochrysis galbana* (Haptophyceae). I. Photosynthetic energy conversion and growth efficiencies. J Phycol 25:462–471

Hessen DO, Anderson TR (2008) Excess carbon in aquatic organisms and ecosystems: physiological, ecological, and evolutionary implications. Limnol Oceanogr 53: 1685–1696

Jones RH, Flynn KJ (2005) Nutritional status and diet composition affect the value of diatoms as copepod prey. Science 307:1457–1459

Keller MD, Kiene RP, Matrai PA, Bellows WK (1999) Production of glycine betaine and dimethylsulfoniopropionate in marine phytoplankton. II. N-limited chemostat cultures. Mar Biol 135:249–257

Kiørboe T (1989) Phytoplankton growth rate and nitrogen content: implications for feeding and fecundity in a herbivorous copepod. Mar Ecol Prog Ser 55:229–234

Klausmeier CA, Litchman E, Daufresne T, Levin SA (2004) Optimal nitrogen-to-phosphorus stoichiometry of phytoplankton. Nature 429:171–174

Klein Breteler WCM, Schogt N, Rampen S (2005) Effect of diatom nutrient limitation on copepod development: role of essential lipids. Mar Ecol Prog Ser 291:125–133

Laws EA (1991) Photosynthetic quotients, new production and net community production in the open ocean. Deep-Sea Res I 38:143–167

Laws EA, Bannister TT (1980) Nutrient- and light-limited growth of *Thalassiosira fluviatilis* in continuous culture, with implications for phytoplankton growth in the ocean. Limnol Oceanogr 25:457–473

Lopez JS, Garcia NS, Talmy D, Martiny AC (2016) Diel variability in the elemental composition of the marine cyanobacterium *Synechococcus.* J Plankton Res 38:1052–1061

Lourenco SO, Barbarino E, Marquez UML, Aidar E (1998) Distribution of intracellular nitrogen in marine microalgae: basis for the calculation of specific nitrogen-to-protein conversion factors. J Phycol 34:798–811

Lund ED, Chu FLE, Harvey E, Adlof R (2008) Mechanism(s) of long chain n-3 essential fatty acid production in two species of heterotrophic protists: *Oxyrrhis marina* and *Gyrodinium dominans.* Mar Biol 155:23–36

MacIntyre HL, Cullen JJ (2005) Using cultures to investigate the physiological ecology of microalgae. In: Andersen RA (ed) Algal culturing techniques. Elsevier Academic Press, Amsterdam, p 287–326

Meï C, Michaud M, Cussac M, Albrieux C and others (2015) Levels of polyunsaturated fatty acids correlate with growth rate in plant cell cultures. Sci Rep 5:15207

Meunier C (2012) You eat what you need: food quality and trophic interactions in planktonic food webs. PhD thesis, Carl Von Ossietzky Universitat, Oldenburg

Mitra A (2006) A multi-nutrient model for the description of stoichiometric modulation of predation in micro- and mesozooplankton. J Plankton Res 28:597–611

Mitra A, Flynn KJ (2005) Predator-prey interactions: Is 'ecological stoichiometry' sufficient when good food goes bad? J Plankton Res 27:393–399

Mitra A, Flynn KJ, Fasham MJR (2007) Accounting for grazing dynamics in the nitrogen-phytoplankton-zooplankton models. Limnol Oceanogr 52:649–661

Montagnes DJS, Lowe CD, Martin L, Watts PC and others (2011) *Oxyrrhis marina* growth, sex and reproduction. J Plankton Res 33:615–627

Morris I (1980) Paths of carbon assimilation in marine phytoplankton. In: Falkowski PG (ed) Primary productivity in the sea. Plenum Press, New York, NY, p 139–159

Pelegrí SP, Dolan J, Rassoulzadegan F (1999) Use of high temperature catalytic oxidation (HTCO) to measure carbon content of microorganisms. Aquat Microb Ecol 16: 273–280

Rhee GY (1978) Effects of N:P atomic ratios and nitrate limitation on algal growth, cell composition, and nitrate uptake. Limnol Oceanogr 23:10–25

Ritchie RJ (2006) Consistent sets of spectrophotometric chlorophyll equations for acetone, methanol and ethanol solvents. Photosynth Res 89:27–41

Roberts EC, Wootton EC, Davidson K, Jeong HJ, Lowe CD, Montagnes DJ (2011) Feeding in the dinoflagellate *O. marina*: linking behavior with mechanisms. J Plankton Res 33:603–614

Russell-Hunter WD (1970) Aquatic productivity. Macmillan Publishers, New York, NY

Shifrin NS, Chisholm SW (1981) Phytoplankton lipids: interspecific differences and effects of nitrate, silicate and light-dark cycles. J Phycol 17:374–384

Shuter B (1979) A model of physiological adaptation in unicellular algae. J Theor Biol 78:519–552

Sterner RW, Elser JJ (2002) Ecological stoichiometry: the biology of elements from molecules to the biosphere. Princeton University Press, Princeton, NJ

Sulkin SD, McKeen GL (1999) The significance of feeding history on the value of heterotrophic microzooplankton as prey for larval crabs. Mar Ecol Prog Ser 186:219–225

Valderrama JC (1981) The simultaneous analysis of total nitrogen and total phosphorus in natural waters. Mar Chem 10:109–122

Wilken S, Hoffman B, Hersch N, Kirchgessner N and others (2011) Diatom frustules show increased mechanical strength and altered valve morphology under iron limitation. Limnol Oceanogr 56:1399–1410

Yang Z, Lowe CD, Crowther W, Fenton A, Watts PC, Montagnes DJ (2013) Strain-specific functional and numerical responses are required to evaluate impacts on predator-prey dynamics. ISME J 7:405–416

Editorial responsibility: Klaus Jürgens, Rostock, Germany

Submitted: November 27, 2017; Accepted: June 25, 2018
Proofs received from author(s): August 16, 2018